

Communication

5,8-Quinolinedione Attached to Quinone Derivatives: XRD Diffraction, Fourier Transform Infrared Spectra and Computational Analysis

Arkadiusz Sokal¹, Roman Wrzalik², Joanna Klimontko² , Elwira Chrobak³ , Ewa Bębenek³ 
and Monika Kadela-Tomanek^{3,*} 

- ¹ Students Scientific Group of Department of Organic Chemistry, Faculty of Pharmaceutical Sciences in Sosnowiec, Medical University of Silesia, Katowice, 4 Jagiellońska Str., 41-200 Sosnowiec, Poland; asokal@outlook.com
- ² Silesian Center for Education and Interdisciplinary Research, Institute of Physics, University of Silesia, 75Pułku Piechoty 1a, 41-500 Chorzów, Poland; roman.wrzalik@us.edu.pl (R.W.); joanna.klimontko@us.edu.pl (J.K.)
- ³ Department of Organic Chemistry, Faculty of Pharmaceutical Sciences in Sosnowiec, Medical University of Silesia, Katowice, 4 Jagiellońska Str., 41-200 Sosnowiec, Poland; echrobak@sum.edu.pl (E.C.); ebebenek@sum.edu.pl (E.B.)
- * Correspondence: mkadela@sum.edu.pl; Tel.: +48-032-364-16-66

Abstract: Quinoline and isoquinoline moieties occur in many natural and synthetic compounds exhibiting high biological activity. The purpose of this study was to analyze the chemical structures of 5,8-quinolinedione and 5,8-isoquinoline derivatives using FT-IR spectroscopy supplemented with theoretical DFT calculations. Spectroscopic measurements were conducted using the attenuated total reflection (ATR) mode in the frequency range of 4000–400 cm⁻¹. An analysis of FT-IR spectra was carried out, assigning the characteristic vibration frequencies of various functional groups to individual peaks. It was found that the experimental and calculated FT-IR spectra showed a good correlation for all the compounds under study. The most significant difference in the spectra occurred in the region of carbonyl bands. For compounds with the 5,8-quinolinedione moiety, two separated C=O vibration peaks were observed, while for compounds with the 5,8-isoquinolinedione moiety, the carbonyl vibrations created only one peak. This difference makes it possible to distinguish between the 5,8-quinolinedione and 5,8-isoquinolinedione derivatives.

Keywords: Fourier transform infrared spectroscopy; 5,8-quinolinedione; DFT



Citation: Sokal, A.; Wrzalik, R.; Klimontko, J.; Chrobak, E.; Bębenek, E.; Kadela-Tomanek, M. 5,8-Quinolinedione Attached to Quinone Derivatives: XRD Diffraction, Fourier Transform Infrared Spectra and Computational Analysis. *Molbank* **2023**, *2023*, M1747. <https://doi.org/10.3390/M1747>

Academic Editor: Rodrigo Abonia

Received: 24 October 2023

Revised: 23 November 2023

Accepted: 24 November 2023

Published: 28 November 2023



Copyright: © 2023 by the authors. Licensee MDPI, Basel, Switzerland. This article is an open access article distributed under the terms and conditions of the Creative Commons Attribution (CC BY) license (<https://creativecommons.org/licenses/by/4.0/>).

1. Introduction

Fourier transform infrared (FT-IR) spectroscopy is a non-destructive technique that can be used to analyze the composition and chemical structure of different compounds [1]. Infrared radiation can be absorbed, transmitted or reflected by a sample to varying degrees depending on how the molecules vibrate when interacting with the radiation. A range from 4000 cm⁻¹ to 400 cm⁻¹ is commonly used to characterize the vibration bands of functional groups in organic compounds [2]. The main advantages of this method are its availability, simplicity, and rapidity, making it very efficient and often used. Moreover, FT-IR spectroscopy allows an analysis of samples in the solid phase, which enables the identification of intermolecular interactions, such as hydrogen bonds. On the other hand, IR spectra are very complicated and their analysis commonly requires the use of a spectral library or theoretical calculations, which is sometimes may limit their use in research [3,4]. Nevertheless, this method is often used in many different fields, from molecular chemistry, microbiology and ecology to food analysis [5–7]. One of the most important methods used during the recording of infrared spectra is the attenuated total reflection (ATR) method, which can be used to obtain infrared spectra from liquid and solid samples. When infrared

light passes through the internal reflection element (IRE), it is reflected back, but at the point where the light hits the surface of a base crystal, an evanescent wave with a certain depth of penetration can be observed within the sample. It interacts with the molecules inside the sample and changes the returning reflected infrared light that is then analyzed. In this method, the depth of penetration can be modified by changing the wavenumber, angle of the infrared light path and IRE due to different materials having different indexes of refraction. Due to the depth of penetration being directly linked to the number of molecules on the path of an evanescent wave, these parameters can be used to modify the sensitivity of ATR [8,9].

Quinoline and isoquinoline moieties occur in many natural and synthetic compounds exhibiting high biological activity, like quinine, quinidine, papaverine, and quiniso-caine [10–13]. The oxidation of quinoline and isoquinoline leads to the obtention of 5,8-quinolinedione and 5,8-isoquinolinedione moieties [14–16]. The recent literature describes the synthesis of many 5,8-quinolinedione and 5,8-isoquinoline compounds containing various substituents in the C-6 and/or C-7 positions. The synthetic compounds exhibited high biological activity, such as anticancer, antibacterial, antimalarial, antifungal and antiviral activity [17–20]. An important issue concerning new compounds is the determination of their molecular structure. In the chemical structure of the 5,8-quinolinedione moiety, there are three hydrogen atoms in the pyridine ring and no hydrogen atoms in the 1,4-quinone moiety. For this reason, the correlation NMR spectra, like HSQC and HMBC, cannot be used to assign carbon atoms in the C-6 and C-7 position. Thus, NMR spectroscopy is not sufficient to determine substitution positions. In this context, FT-IR spectroscopy has been shown to be a useful technique to identify the position of the substituent in the 5,8-quinolinedione moiety [21–27]. In the analysis of the FT-IR spectra, the carbonyl wavelength range of $1700\text{--}1650\text{ cm}^{-1}$ is the most important. For compounds with amine, the group in the C-6 position, only one peak in this area is observed, while for the 7-amine substituent derivatives, two separated peaks can be seen [22,24]. However, studies conducted on 5,8-isoquinolinedione via infrared spectroscopy (IR) are very scarce in the literature [28].

In this study, we used Fourier transform infrared spectroscopy (FT-IR) to analyze the chemical structures of 5,8-quinolinedione (1,2) and 5,8-isoquinolinedione (3,4) derivatives (Figure 1). The crystal structure of compounds 1–4 was confirmed via the X-ray diffraction technique (XRD). The analysis was supplemented with the theoretical spectra obtained using density functional theory (DFT) calculations. The DFT method was used to construct the molecular potential maps (MEP). MEP analysis allows for the localization of the nucleophilic and electrophilic areas within a molecule.

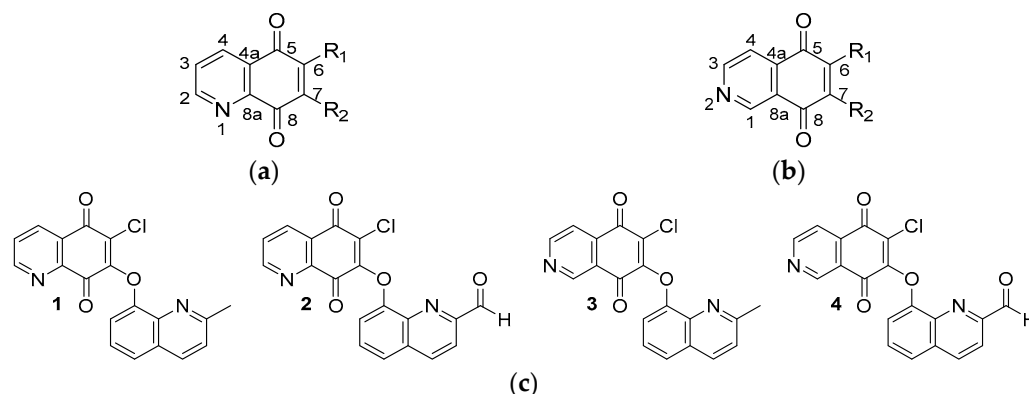


Figure 1. The chemical structures of (a) 5,8-quinolinedione, (b) 5,8-isoquinolinedione and (c) its derivatives 1–4.

2. Results

2.1. Analysis of Molecular Structure

X-ray diffraction (XRD) is a useful tool with which to obtain information about the crystal structure of powdered compounds. Figure 2 presents the XRD pattern for the tested compounds, 1–4, in a 2θ angle range from 5° to 40° .

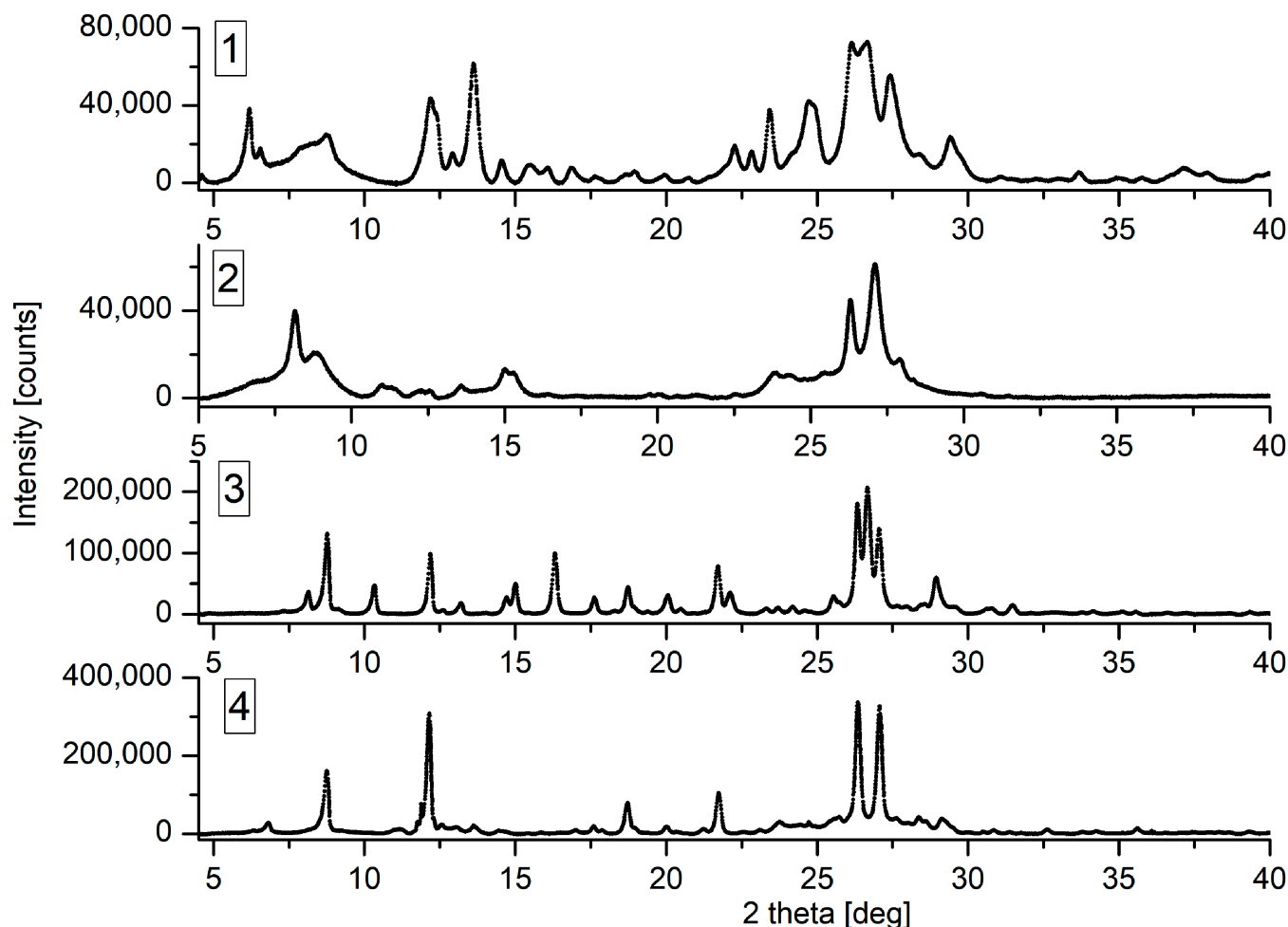


Figure 2. The XRD pattern of compounds 1–4 in a 2θ angle range from 5° to 40° .

The XRD patterns of all compounds reveal sharp diffraction peaks, indicating the presence of a well-crystallized fraction [29]. According to the literature, the width of the peak is related to the crystallite's size [30]. The broad peaks (FWHM, full width at half maximum; the values are 0.7° to 1.1°), like they do in XRD patterns of 5,8-quinolinedione derivatives 1 and 2, indicate the small size of crystallites, while the sharp peaks (FWHM; values are 0.2° to 0.5°), of 5,8-isoquinolinedione 3 and 4, indicate their larger size.

The Scherrer equation was used to estimate the average crystalline particle size from the peaks in the range 20.0° to 32.0° . The values are from about 10 nm to 15 nm for 5,8-quinolinedione derivatives 1 and 2, and 25 nm to 40 nm for 5,8-isoquinolinedione 3 and 4, respectively.

Based on the various studies of a single-crystal XRD pattern, the highest peaks in diffractograms have been analyzed [21,26,31,32]. The peaks in the range of 26.14° – 27.06° are assigned to the 5,8-quinolinedione moiety (Figure S1). For the compound with the 5,8-quinolinedione moiety (1 and 2), the distance between these peaks is greater than that for 5,8-isoquinolinedione derivatives (3 and 4) and is in the range from 0.53 to 0.77 and from 0.34 to 0.73 , respectively (Figures 2 and S1). The same correlation was observed for crystal structures described in the literature [21,31,32]. Comparing the diffractogram shows

that peak at 27.43° and 29.40° , and 27.04° and 28.95° belong to a 2-methyl-8-quinolinoxy substituent in compound **1** and **3**, respectively.

In the next step, we analyzed the DFT (B3LYP/6-311G++(d,p))-optimized structures of quinone derivatives (Figure 3). The angles between planes containing the 5,8-quinolinedione (**1–2**) or 5,8-isoquinolinedione (**3–4**) moiety and the quinoline substituent are in the range from 69.42° to 78.83° . The results show that the type of 5,8-quinolinedione moiety slightly influences the arrangement of compounds **1–4**. The calculated bond lengths and angles for **1–4** are shown in Tables S1–S4. Comparing the C–C, C–N and C–O bond lengths in the 5,8-quinolinedione and quinoline moieties shows that the π electrons are delocalized throughout the molecule.

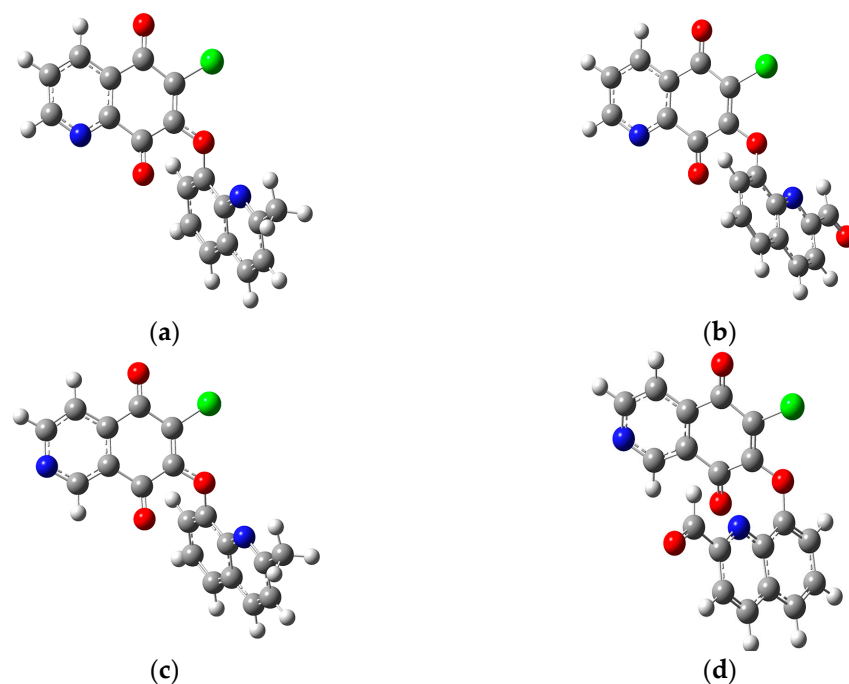


Figure 3. The optimized structures of compounds (a) **1**; (b) **2**; (c) **3**; (d) **4**.

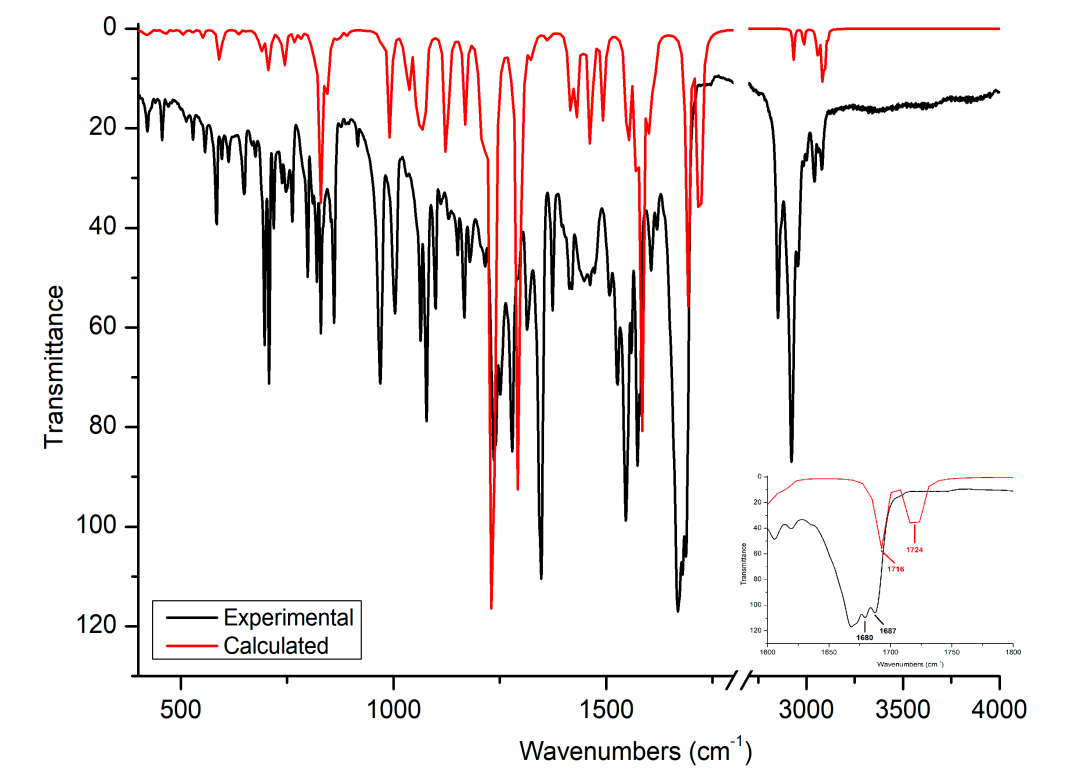
2.2. FT-IR Spectra

Figure 4 presents the experimental and calculated spectra for compounds **1–4**. Comparing the experimental and predicted spectra reveals a good fit.

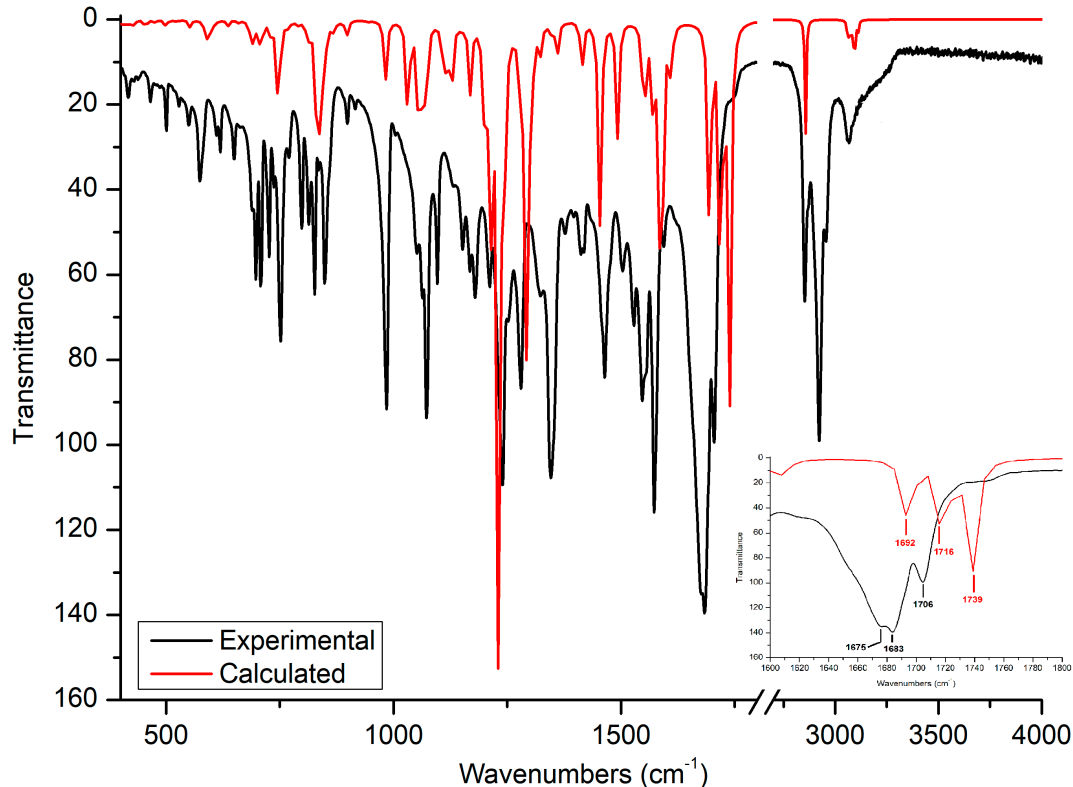
Table 1 presents the bands assignments for experimental and calculated vibrations.

2.2.1. C–C and C–H Vibrations

The stretching vibration of the C–H groups of 5,8-quinolinedione and quinoline rings are observed to be in the ranges of $3087\text{--}2852\text{ cm}^{-1}$ and $3112\text{--}2850\text{ cm}^{-1}$ in experimental and calculated spectra, respectively. In the calculated spectra of compounds **2** and **4**, a peak at $2857\text{--}2850\text{ cm}^{-1}$ is observed, which is attributed to the stretching vibrations of the C–H aldehyde group. In the experimental spectrum, this band is overlapped by other C–H vibrations of the quinoline ring (Figure 2). According to the calculated spectra, the strong band at $1668\text{--}1582\text{ cm}^{-1}$ is attributed mainly to the C–C vibration of the C6–C7 atoms. The absorption peaks in the ranges of $1617\text{--}1507\text{ cm}^{-1}$ and $1473\text{--}1374\text{ cm}^{-1}$ are attributed to the C–C and C–H stretching vibrations of the 5,8-quinolinedione and quinoline rings, respectively. The deformation vibration of the C–H and C–C groups of the 5,8-quinolinedione and quinoline rings are observed in the range of $1106\text{--}969\text{ cm}^{-1}$ (Table 1).

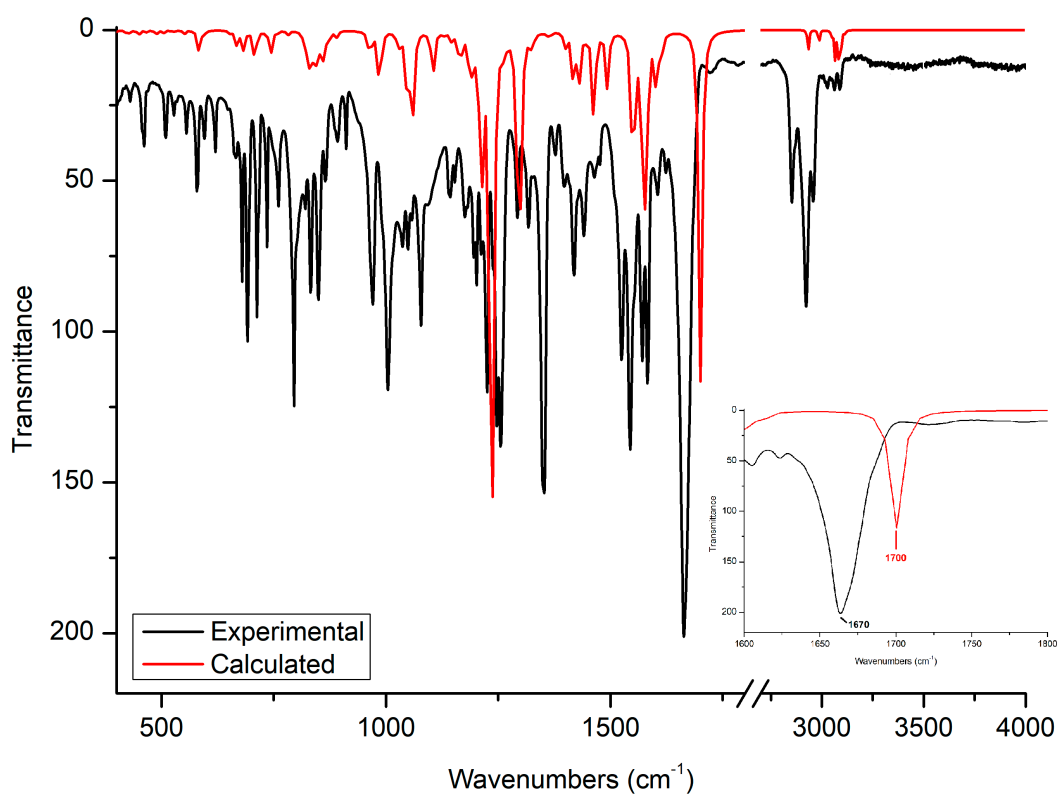


(a)

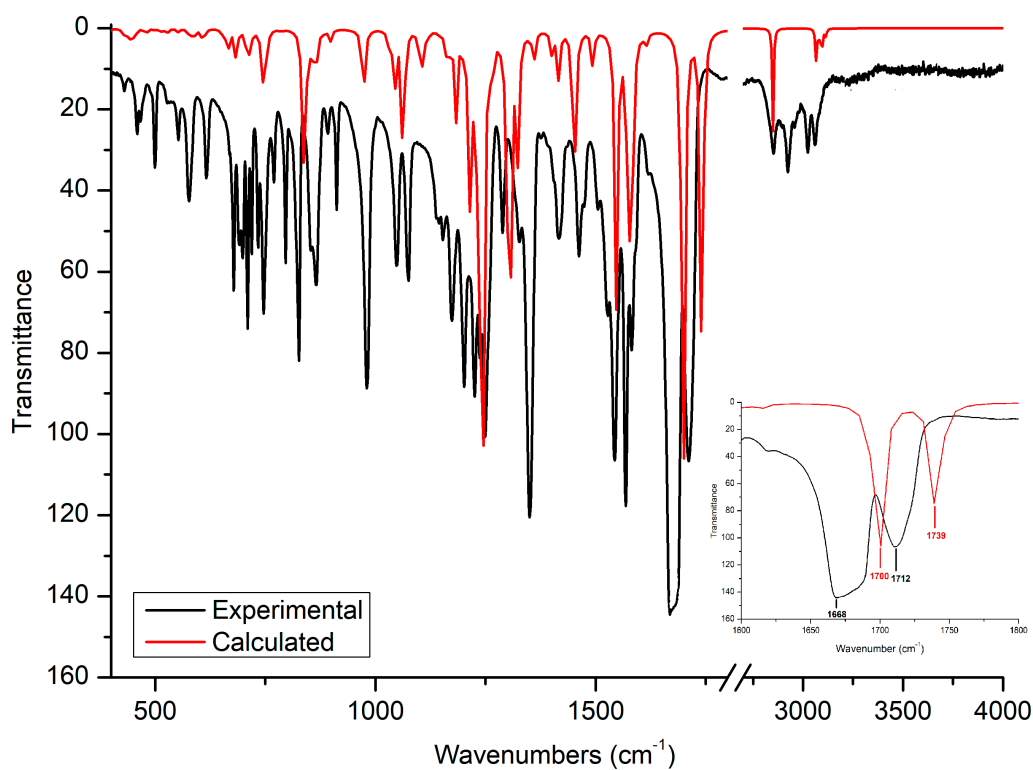


(b)

Figure 4. Cont.



(c)



(d)

Figure 4. Experimental (black line) and calculated (red line) FT-IR spectra recorded in the range of 400–4000 cm⁻¹ for (a) 1, (b) 2, (c) 3 and (d) 4.

Table 1. Band assignments of experimental and calculated FT-IR spectra for 1–4.

Assignment	1		2		3		4	
	Exp	Calc	Exp	Calc	Exp	Calc	Exp	Calc
v C–H 5,8-quinolinedione and quinoline	3081–2852	3096–2934	3068–2852	3112 2857	3087–2853	3081–2934	3058–2853	3112 2850
v C=O	-	-	1706	1739	-	-	1712	1739
v _{as} C=O	1687	1724	1683	1716	1670	1700	1668	1700
v _s C=O	1680	1716	1675	1692	1582	1577	1582	1577
v C–C 5,8-quinolinedione	1668	1692	1584	1572	1570–1524	1546	1583–1534	1546
v C–C, C–H 5,8-quinolinedione	1617–1507	1600–1553	1556–1527	1569–1546	1477–1396	1491–1415	1492–1415	1492–1415
v C–C, C–H quinoline	1473–1374	1492–1415	1464–1411	1492–1415	1318	1322	1325	1322
v C–N quinoline	1314	1322	1321	1322	1292	1299	1288	1307
v C–O 5,8-quinolinedione	1278	1291	1281	1291	1256–1247	1237	1248–1237	1245
v C–N 5,8-quinolinedione	1236	1230	1239	1230	1106–983	1075–891	1106–898	
δ C–C, C–H 5,8-quinolinedione and quinoline	1166–969	1168–991	1178–984	1168–983	833	829	826	836
v C–Cl	829	829	826	836				

2.2.2. C–N and C–O Vibrations

According to the literature [33,34], the C–O vibration in the ether is located in the range of 1275–1200 cm⁻¹. For tested compounds, this vibration of an ether is observed in the range of 1307–1278 cm⁻¹ (Table 1). The observed shift towards higher wavenumbers may be due to the delocalization of π electrons throughout the molecule.

The derivatives 1–4 contain two nitrogen atoms. An analysis of the calculated spectra shows that the stretching vibrations of C–N in the quinoline and 5,8-quinolinedione moieties are observed at the 1325–1314 cm⁻¹ and 1256–1230 cm⁻¹ frequencies, respectively. For compounds 3–4, which contain the 5,8-isoquinolinedione moiety, the C–N vibration peak in the 5,8-isoquinolinedione moiety is split into two separate peaks (Table 1).

2.2.3. C=O Vibrations

The 5,8-quinolinedione moiety contains two carbonyl groups in the C-5 and C-8 positions. According to the data in the literature, these two groups create two separate peaks in the region of 1638–1704 cm⁻¹. The asymmetric vibration at higher wavenumbers is attributed mainly to the carbonyl group in the C-8 position, while the symmetric vibration is attributed mainly to the carbonyl group in the C-5 position [23–27]. The same trend is observed for compounds 1–2. Comparing the calculated and experimental spectra reveals that the C=O vibrations are shifted towards lower wavenumbers from 1724–1716 cm⁻¹ to 1687–1683 cm⁻¹ and from 1692–1716 cm⁻¹ to 1675–1680 cm⁻¹ for asymmetric (ν_a) and symmetric (ν_s) stretching vibrations, respectively. The frequency band separation ($\Delta\nu = \nu_a - \nu_s$) in the calculated spectra depends on the type of quinoline substituent in the C-7 position of the 5,8-quinolinedione moiety. The $\Delta\nu$ is equal to 7 cm⁻¹ and 24 cm⁻¹ for compounds 1 and 2, respectively, while in the experimental spectrum this separation is slightly different and is 7 cm⁻¹ and 8 cm⁻¹ for 1 and 2, respectively. Comparing the spectra of 5,8-quinolinedione (1–2) and 5,8-isoquinolinedione (3–4) compounds reveals that for 3–4, only one C=O vibration peak is observed. In this case, the asymmetric and symmetric vibrations are not split (Figure 2).

Additionally, for compounds 2 and 4, a peak at 1712–1706 cm⁻¹ is seen and can be assigned to the aldehyde group in the C-2 position of the quinoline moiety.

2.2.4. C–Cl Vibrations

The C–Cl vibrations are difficult to identify because the peaks are usually observed to be in the range of 760–505 cm^{-1} [33,34]. The analysis of the calculated vibrations shows that the C–Cl stretching vibrations occur at 836–829 cm^{-1} . In the experimental spectra, this band is slightly shifted towards lower wavenumbers of 829–826 cm^{-1} .

2.3. Molecular Electrostatic Potential Maps

The molecular properties of a compound depend on the type of heteroatoms and their arrangement in the structure of the molecule. One of the most important properties is charge distribution, which describes the nucleophilic and electrophilic regions in the molecule [35,36]. A molecular electrostatic potential map (MEP) is a graphical representation of charge distribution. The MEP maps of compounds 1–4 were constructed using the DFT/B3LYP level with the 6-311G++(d,p) basis set, and they were sketched for an order of -29.413 kcal/mol to 29.413 kcal/mol. The red color represents the nucleophilic region, blue represents the electrophilic region and green represents the neutral region. The MEP maps are presented in Figure 5a–d.

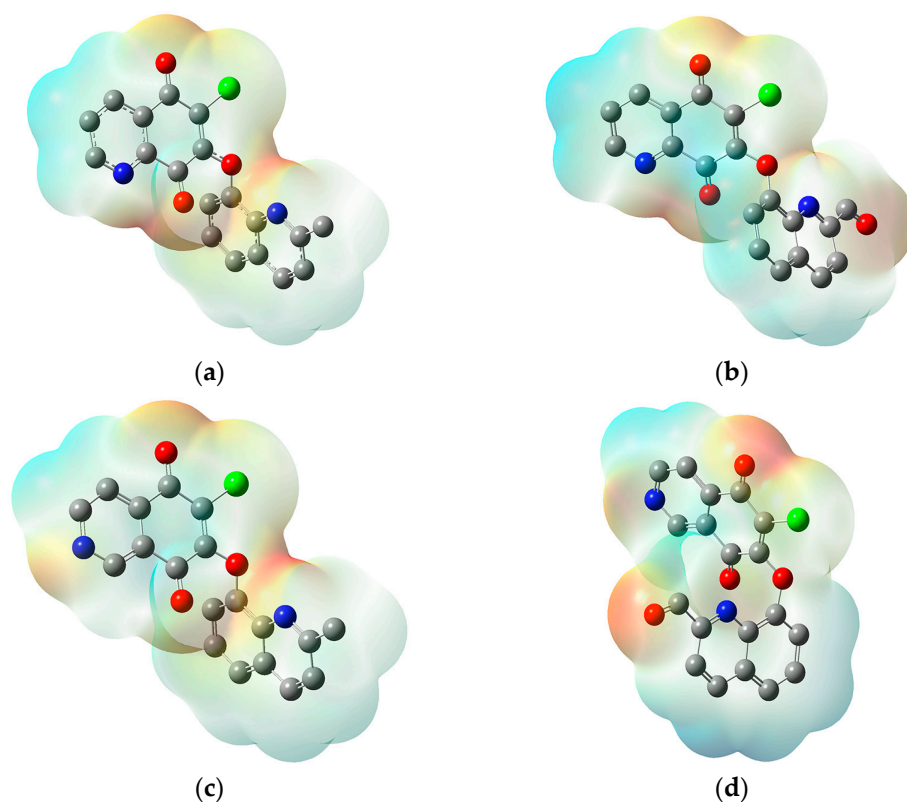


Figure 5. Molecular electrostatic potential plotted for compounds (a) 1, (b) 2, (c) 3 and (d) 4.

For all molecules, the nucleophilic regions are localized near the oxygen atoms in the C-5, C-6 and C-8 positions and nitrogen atoms in 5,8-quinolinedione and quinoline moieties. Additionally, for 3 and 4, a nucleophilic region near the oxygen atom in the carbonyl group is observed. The value of local potential minima was determined for all nucleophilic regions (Table S5). For all derivatives, the value of the local minimum in the area containing the oxygen atom in the C-5 position of the 5,8-quinolinedione moiety is in the range from -1.74 eV to -1.96 eV. For compounds 1 and 2, two local minima in the ranges from -1.44 eV to -1.61 eV and from -1.42 eV to -1.58 eV, respectively, in the area near the oxygen atom in the C-8 position are observed. In this area, for the compound with the 5,8-isoquinolinedione moiety (3 and 4), only one local minimum (-1.47 eV and -1.20 eV, respectively) is observed. The value of the local potential minimum in the area

near the oxygen atom in the C-6 position depends on the type of quinoline substituent. For compounds with the 2-methylquinoline moiety (**1** and **3**), it is equal to -1.20 eV and -1.09 eV, respectively, while for **2** and **4**, it is equal to -0.93 eV and -0.82 eV, respectively. Two negative areas are located near the nitrogen atoms. The first of them contains a nitrogen atom in the 5,8-quinolinedione moiety, and the second one contains a nitrogen atom in the quinoline fragment. The local minima in these areas are in the range from -2.12 eV to -2.39 eV and from -2.23 eV to -2.72 eV. Additionally, for compounds **2** and **3**, a local minimum near the oxygen atom at the carbonyl group, equal to -1.74 eV and -1.77 eV, respectively, can be observed.

The electrophilic regions for all molecules are localized near the hydrogen atoms in the 5,8-quinolinedione and quinoline moieties. The charge-neutral regions contain carbons rings of both moieties and a chloride atom. Moreover, the hydrogen atom in the C-1 position in the 5,8-isoquinolinedione moiety (**3** and **4**) is charge-neutral.

3. Materials and Methods

3.1. Synthesis

The synthesis of compounds **1–4** (Figure 1) was described in the literature [20]. Briefly, the 6,7-dichloro-5,8-quinolinedione (1 mmol) or 6,7-dichloro-5,8-isoquinolinedione (1 mmol) was dissolved in tetrahydrofuran (2 mL). Then, the 2-methylquinolin-8-ol (1.2 mmol) or 8-hydroxyquinoline-2-carbaldehyde (1.2 mmol) and potassium carbonate (1 mmol) were added. After 24 h in room temperature, the reaction mixture was concentrated in a vacuum evaporator. Purification via column chromatography (SiO₂, chloroform/ethanol, 15:1, *v/v*) gave pure products with a yield of 52–67%.

3.2. Physical Measurements

The XRD measurements were carried out using a high-resolution PANalytical Empyrean diffractometer with CuK α radiation (40 kV, 30 mA) equipped with the PIXcel detector. The diffraction patterns were collected using the 2θ scan from 5° to 80° with 0.0131° steps. Data analysis was carried out using the HighScore Plus 4.6 software supplied by PANalytical.

The FT-IR spectrometer Nicolet iS50 (Thermo Fisher Scientific, Waltham, MA, USA) equipped with the attenuated total reflection (ATR) diamond accessory MIRacle (PIKE Technology, Fitchburg, WI, USA) was used for measurement. In total, 64 scans were accumulated with a resolution of 2 cm^{-1} (digital resolution 0.482 cm^{-1}) in the spectral range of $4000\text{--}400\text{ cm}^{-1}$. To calculate absorbance, ATR correction was used to transform the reflectance spectrum into a $\log(1/R)$ absorption spectrum (the refractive index value was assumed to be 1.45 for all tested substances).

3.3. Computational Details

The molecular structures of compounds **1–4** were optimized via the DFT (B3LYP/6-) using the Gaussian 16 package [37]. The IR spectra calculations were performed for the optimized geometries at the same level of the theory (B3LYP/6-311G++(d,p)); all harmonic frequencies were real numbers. The theoretical peak positions were scaled by a factor of 0.964 [38] to compare the calculated spectra with the experimental ones. The calculated structures of molecules were used to determine the molecular surface, which is defined as an arrangement of the electrostatic potential $V(r)$ on the electron density maps [39]. We visualized all obtained results using the GaussView, Version 5, software package [40].

4. Conclusions

The crystal structure of derivatives **1–4** were characterized according to their XRD pattern. The analysis show that the size of crystallites depends on the type of 5,8-quinolinedione moiety. The size of crystallites for the derivatives of 5,8-quinolinedione **1** and **2** is equal to 10 nm to 15 nm, respectively, while that for 5,8-isoquinolinedione **3** and **4** is equal to 25 nm to 40 nm, respectively.

The experimental and calculated FT-IR spectra showed a good correlation for all compounds, 1–4. The most significant difference in the spectra of studied compounds occurred in the region of the carbonyl bands. For compounds with the 5,8-quinolinedione moiety (1–2), two separated peaks were observed. In the experimental spectrum, the separation of the carbonyl bands is not dependent on the type of quinoline substituent. For compounds 3–4 with the 5,8-isoquinolinedione moiety, the carbonyl vibrations create only one peak. Based on this difference, it can be concluded that the frequency region of 1700–1650 cm^{-1} allows us to distinguish between the 5,8-quinolinedione and 5,8-isoquinolinedione derivatives.

The molecular potential maps show that the charge distribution depends on the type of 5,8-quinolinedione moiety. The most important difference is observed in the nucleophilic region near the oxygen atom in the C-8 position. In this area, for compounds with a 5,8-quinoline moiety, two local potential minima were observed, while for derivatives with a 5,8-isoquinoline moiety, there was only one.

Supplementary Materials: Figure S1. The XRD pattern of compounds 1–4 in a 2θ angle range from 25° to 30° ; Table S1. Geometric parameters (bond length and angles) for compound 1 (\AA , $^\circ$); Table S2: Geometric parameters (bond length and angles) for compound 2 (\AA , $^\circ$); Table S3: Geometric parameters (bond length and angles) for compound 3 (\AA , $^\circ$); Table S4: Geometric parameters (bond length and angles) for compound 4 (\AA , $^\circ$); Table S5. The value of local potential minima for nucleophilic regions in compounds 1–4.

Author Contributions: Conceptualization and writing—original draft preparation, M.K.-T.; methodology and writing—original draft preparation, A.S.; methodology, R.W. and J.K.; formal analysis, E.B. and E.C. All authors have read and agreed to the published version of the manuscript.

Funding: This research was funded by the Medical University of Silesia in Katowice, Poland, Grant PCN-2-027/K/2/F.

Data Availability Statement: Samples of compounds 1–4 are available from the authors.

Conflicts of Interest: The authors declare no conflict of interest.

References

1. Barnes, M.; Sulé-Suso, J.; Millett, J.; Roach, P. Fourier transform infrared spectroscopy as a non-destructive method for analysing herbarium specimens. *Biol. Lett.* **2023**, *19*, 20220546. [[CrossRef](#)] [[PubMed](#)]
2. Geraldes, C.F.G.C. Introduction to infrared and raman-based biomedical molecular imaging and comparison with other modalities. *Molecules* **2020**, *25*, 5547. [[CrossRef](#)] [[PubMed](#)]
3. Zhang, J.; Zhou, Q.; Zhang, D.; Yang, G.; Zhang, C.; Wu, Y.; Xu, Y.; Chen, J.; Kong, W.; Kong, G.; et al. The agronomic traits, alkaloids analysis, FT-IR and 2DCOS-IR spectroscopy identification of the low-nicotine-content nontransgenic tobacco edited by CRISPR-Cas9. *Molecules* **2022**, *27*, 3817. [[CrossRef](#)] [[PubMed](#)]
4. Krysa, M.; Szymańska-Chargot, M.; Zdunek, A. FT-IR and FT-Raman fingerprints of flavonoids—A review. *Food Chem.* **2022**, *393*, 133430. [[CrossRef](#)] [[PubMed](#)]
5. Koczoń, P.; Hołaj-Krzak, J.T.; Palani, B.K.; Bolewski, T.; Dąbrowski, J.; Bartyzel, B.J.; Gruczyńska-Sękowska, E. The analytical possibilities of FT-IR spectroscopy powered by vibrating molecules. *Int. J. Mol. Sci.* **2023**, *24*, 1013. [[CrossRef](#)] [[PubMed](#)]
6. Passaris, I.; Mauder, N.; Kostrzewa, M.; Burckhardt, I.; Zimmermann, S.; van Sorge, N.M.; Slotved, H.C.; Desmet, S.; Ceysens, P.J. Validation of fourier transform infrared spectroscopy for Serotyping of *Streptococcus pneumoniae*. *J. Clin. Microbiol.* **2022**, *60*, 0032522. [[CrossRef](#)] [[PubMed](#)]
7. Sala, A.; Cameron, J.M.; Jenkins, C.A.; Barr, H.; Christie, L.; Conn, J.J.A.; Evans, T.R.J.; Harris, D.A.; Palmer, D.S.; Rinaldi, C.; et al. Liquid Biopsy for Pancreatic Cancer Detection Using Infrared Spectroscopy. *Cancers* **2022**, *14*, 3048. [[CrossRef](#)]
8. Milosevic, M. Internal Reflection and ATR Spectroscopy. *Appl. Spectrosc. Rev.* **2004**, *39*, 365–384. [[CrossRef](#)]
9. Cui, L.; Butler, H.J.; Martin-Hirsch, P.L.; Martin, F.L. Aluminium Foil as a Potential Substrate for ATR-FTIR, Transfection FTIR or Raman Spectrochemical Analysis of Biological Specimens. *Anal. Methods* **2016**, *8*, 481–487. [[CrossRef](#)]
10. Guan, Y.F.; Liu, X.J.; Yuan, X.Y.; Liu, W.B.; Li, Y.R.; Yu, G.X.; Tian, X.Y.; Zhang, Y.B.; Song, J.; Li, W.; et al. Design, synthesis, and anticancer activity studies of novel quinoline-chalcone derivatives. *Molecules* **2021**, *26*, 4899. [[CrossRef](#)]
11. Patel, K.B.; Kumari, P. A review: Structure-activity relationship and antibacterial activities of quinoline based hybrids. *J. Mol. Struct.* **2022**, *1268*, 133634. [[CrossRef](#)]
12. Mohan, I.; Ayyakannu, A.N. Review on recent development of quinoline for anticancer activities. *Arab. J. Chem.* **2022**, *15*, 104168.

13. Hu, S.; Chen, J.; Cao, J.X.; Zhang, S.S.; Gu, S.; Chen, F. Quinolines and isoquinolines as HIV-1 inhibitors: Chemical structures, action targets, and biological activities. *Bioorg. Chem.* **2023**, *136*, 106549. [[CrossRef](#)] [[PubMed](#)]
14. Boger, D.; Yasuda, M.; Mitscher, L.; Drake, S.; Kitos, P.; Thompson, S. Streptonigrin and lavendamycin partial structures. Probes for the minimum, potent pharmacophore of streptonigrin, lavendamycin, and synthetic quinoline-5,8-diones. *J. Med. Chem.* **1987**, *30*, 1918–1928. [[CrossRef](#)] [[PubMed](#)]
15. Bringmann, G.; Reichert, Y.; Kane, V. The total synthesis of streptonigrin and related antitumor antibiotic natural products. *Tetrahedron* **2004**, *60*, 3539–3574. [[CrossRef](#)]
16. El Shehry, M.F.; Ghorab, M.M.; Abbas, S.Y.; Fayed, E.A.; Shedid, S.A.; Ammar, Y.A. Quinoline derivatives bearing pyrazole moiety: Synthesis and biological evaluation as possible antibacterial and antifungal agents. *Eur. J. Med. Chem.* **2018**, *142*, 1463–1473. [[CrossRef](#)]
17. Kadela-Tomanek, M.; Bębenek, E.; Chrobak, E.; Boryczka, S. 5,8-Quinolinedione scaffold as a promising moiety of bioactive agents. *Molecules* **2019**, *24*, 4115. [[CrossRef](#)]
18. Mancini, I.; Vigna, J.; Sighel, D.; Defant, A. Hybrid molecules containing naphthoquinone and quinolinedione scaffolds as antineoplastic agents. *Molecules* **2022**, *27*, 4948. [[CrossRef](#)]
19. Guo, K.; Li, J.; Jia, Y.; Yang, X.; Yan, X.; Wu, L. Design, synthesis, and biological evaluation of quinolinedione-linked sulfonylpiperazine derivatives as NQO1-directed antitumor agents. *Bioorg. Chem.* **2023**, *132*, 106385. [[CrossRef](#)]
20. Kadela-Tomanek, M.; Jastrzębska, M.; Chrobak, E.; Bębenek, E.; Latocha, M. Hybrids of 1,4-quinone with quinoline derivatives: Synthesis, biological activity, and molecular docking with DT-Diaphorase (NQO1). *Molecules* **2022**, *27*, 6206. [[CrossRef](#)]
21. Lee, D.; Ko, J.; Lee, K. Cesium carbonate-mediated reaction of dichloronaphthoquinone derivatives with O-nucleofiles. *Monatsh. Chem.* **2007**, *138*, 741–746. [[CrossRef](#)]
22. Yoon, E.; Choi, H.; Shin, K.; Yoo, K.; Chi, D.; Kim, D. The regioselectivity in the reaction of 6,7-dihaloquinoline-5,8-diones with amine nucleophiles in various solvents. *Tetrahedron Lett.* **2000**, *41*, 7475–7480. [[CrossRef](#)]
23. Kadela-Tomanek, M.; Jastrzębska, M.; Chrobak, E.; Bębenek, E.; Latocha, M.; Kusz, J.; Boryczka, S. Structural and spectral characterization of 2-amino-2H-[1,2,3]triazolo[4,5-g]quinoline-4,9-dione polymorphs. Cytotoxic activity and molecular docking study with NQO1 enzyme. *Spectrochim. Acta A Mol. Biomol. Spectrosc.* **2020**, *230*, 118038. [[CrossRef](#)] [[PubMed](#)]
24. Jastrzębska, M.; Boryczka, S.; Kadela, M.; Wrzalik, R.; Kusz, J.; Nowak, M. Synthesis, crystal structure and infrared spectra of new 6- and 7-propylamine-5,8-quinolinediones. *J. Mol. Struct.* **2014**, *1067*, 160–168. [[CrossRef](#)]
25. Kadela-Tomanek, M.; Jastrzębska, M.; Marciniak, K.; Chrobak, E.; Bębenek, E.; Boryczka, S. Lipophilicity, pharmacokinetic properties, and molecular docking study on SARS-CoV-2 target for betulin triazole derivatives with attached 1,4-quinone. *Pharmaceutics* **2021**, *13*, 781. [[CrossRef](#)] [[PubMed](#)]
26. Kadela-Tomanek, M.; Pawełczak, B.; Jastrzębska, M.; Bębenek, E.; Chrobak, E.; Latocha, M.; Kusz, J.; Książek, M.; Boryczka, S. Structural, vibrational and quantum chemical investigations for 6,7-dichloro-2-methyl-5,8-quinolinedione. Cytotoxic and molecular docking studies. *J. Mol. Struct.* **2018**, *1168*, 73–83. [[CrossRef](#)]
27. Kadela-Tomanek, M.; Jastrzębska, M.; Bębenek, E.; Chrobak, E.; Latocha, M.; Kusz, J.; Tarnawska, D.; Boryczka, S. New acetylenic amine derivatives of 5,8-quinolinediones: Synthesis, crystal structure and antiproliferative activity. *Crystals* **2017**, *7*, 15. [[CrossRef](#)]
28. Kubo, A.; Kitahara, Y.; Nakahara, S.; Numata, R. The ceric ammonium nitrate mediated synthesis of quinoline and isoquinoline quinones. *Chem. Pharm. Bull.* **1983**, *31*, 341–343. [[CrossRef](#)]
29. Fizer, O.; Fizer, M.; Filep, M.; Sidey, V.; Mariychuk, R. On the structure of cetylpyridinium perchlorate: A combined XRD, NMR, IR and DFT study. *J. Mol. Liq.* **2022**, *368*, 120659. [[CrossRef](#)]
30. Raja, P.B.; Munusamy, K.R.; Perumal, V.; Ibrahim, M.N.M. 5—Characterization of nanomaterial used in nanobioremediation. In *Micro and Nano Technologies, Nano-Bioremediation: Fundamentals and Applications*; Iqbal, H.M.N., Bilal, M., Nguyen, T.A., Eds.; Elsevier: Amsterdam, The Netherlands, 2022.
31. Kadela, M.; Jastrzębska, M.; Bębenek, E.; Chrobak, E.; Latocha, M.; Kusz, J.; Książek, M.; Boryczka, S. Synthesis, structure and cytotoxic activity of mono- and dialkoxy derivatives of 5,8-quinolinedione. *Molecules* **2016**, *21*, 156. [[CrossRef](#)]
32. Kadela-Tomanek, M.; Jastrzębska, M.; Pawełczak, B.; Bębenek, E.; Chrobak, E.; Latocha, M.; Książek, M.; Kusz, J.; Boryczka, S. Alkynyloxy derivatives of 5,8-quinolinedione: Synthesis, in vitro cytotoxicity studies and computational molecular modeling with NAD(P)H:Quinone oxidoreductase 1. *Eur. J. Med. Chem.* **2017**, *126*, 969–982. [[CrossRef](#)]
33. Socrates, G. *Infrared and Raman Characteristic Group Frequencies*, 3rd ed.; Wiley-Blackwell: Hoboken, NJ, USA, 2004.
34. Silverstein, R.; Webster, F.; Kiemle, D.; Bryce, D. *Spectrometric Identification of Organic Compounds*, 8th ed.; Wiley: New York, NY, USA, 2014.
35. Chandrasekaran, K.; Kumar, R. Structural, spectral, thermodynamical, NLO, HOMO, LUMO and NBO analysis of fluconazole. *Spectrochim. Acta A* **2015**, *150*, 974. [[CrossRef](#)]
36. Vennila, M.; Rathikha, R.; Muthu, S.; Jeelani, A.; Irfan, A. Theoretical structural analysis (FT-IR, FT-R), solvent effect on electronic parameters NLO, FMO, NBO, MEP, UV (IEFPCM model), Fukui function evaluation with pharmacological analysis on methyl nicotinate. *Comput. Theor. Chem.* **2022**, *1217*, 113890. [[CrossRef](#)]
37. Frisch, M.J.; Trucks, G.W.; Schlegel, H.B.; Scuseria, G.E.; Robb, M.A.; Cheeseman, J.R.; Scalmani, G.; Barone, V.; Mennucci, B.; Petersson, G.A.; et al. Gaussian 16, Revision A. 03. In *GaussView 5.0*; Gaussian, Inc.: Wallingford, CT, USA, 2016.
38. Foresman, J.B.; Frisch, A.E. *Exploring Chemistry with Electronic Structure Methods: A Guide to Using Gaussian*, 3rd ed.; Gaussian, Inc.: Wallingford, CT, USA, 2015; ISBN 978-1-935522-03-4.

39. Politzer, P.; Laurence, P.; Jayasuriya, K. Molecular electrostatic potentials: An effective tool for the elucidation of biochemical phenomena. *Environ. Health Perspect.* **1985**, *61*, 191–202. [[CrossRef](#)]
40. Dennington, R.; Keith, T.; Millam, J. *GaussView, Version 5*; Semichem Inc.: Shawnee Mission, KS, USA, 2009.

Disclaimer/Publisher's Note: The statements, opinions and data contained in all publications are solely those of the individual author(s) and contributor(s) and not of MDPI and/or the editor(s). MDPI and/or the editor(s) disclaim responsibility for any injury to people or property resulting from any ideas, methods, instructions or products referred to in the content.